Journal of Holistic Integrative Pharmacy 6 (2025) 11–22

Contents lists available at ScienceDirect

Journal of Holistic Integrative Pharmacy

journal homepage: www.keaipublishing.com/en/journals/journal-of-holistic-integrative-pharmacy

The repair effect of α-ketoglutarate combined with mesenchymal stem cells on osteoarthritis via the hedgehog protein pathway

Liyan Li, Han Shen *, Li Lu **

College of Life Sciences and Biopharmaceuticals, Guangdong Pharmaceutical University, Guangzhou, 510006, China

ARTICLE INFO

Keywords:
Mesenchymal stem cell
Aging
Osteoarthritis
Hedgehog
Articular cartilage

ABSTRACT

Objective: Mesenchymal stem cell (MSC) therapy represents a promising treatment strategy for osteoarthritis (OA). Nevertheless, the therapeutic efficacy of MSCs may be attenuated under conditions of cellular senescence or when the available clinical quantity is insufficient. α-Ketoglutarate (AKG) exerts beneficial effects on skeletal tissues and the activity of stem cells. Consequently, the present study was designed to explore the potential of AKG in augmenting the viability of MSCs and the potential of their combined utilization in the treatment of OA.

Methods: MSCs with senescence induced by *in vitro* passaging served as the experimental subjects. The effects of AKG on the activity of senescent MSCs were investigated via morphological observation, scratch assay, and DAPI staining. Bioinformatics methods were employed to explore the action targets and pathways of AKG in the treatment of OA, providing a theoretical basis and experimental evidence for further experiments. The feasibility of this pathway was verified at the animal level. A rat model of OA was induced by intra-articular injection of sodium monoiodoacetate (MIA). Platelet-rich plasma (PRP), a representative drug for clinical OA treatment, was used as a positive control. The efficacy of combined high-dose and low-dose medications was evaluated through morphological observation and pathological section staining.

Results: The outcomes of the *in vitro* cellular experiments indicate that AKG is capable of decreasing the quantity of MSCs exhibiting senescent morphological features, enhancing the migratory capacity of MSCs, and suppressing the apoptotic process of MSCs. Consequently, AKG exerts a reparative influence on senescent MSCs. Bioinformatics analysis indicated that AKG exerts its repairing effect on OA by inhibiting the Hedgehog (HH) signaling pathway. Additionally, at the animal experiment level, we found that the synergistic effect of high-dose AKG combined with MSCs could more significantly alleviate the severity of OA. It enhances matrix synthesis, reduces endochondral ossification, and promotes cartilage repair through the HH pathway.

Conclusion: Our research indicates that AKG has a significant effect on enhancing the activity of MSCs. The combined treatment can promote the repair of articular cartilage in OA rats through the HH pathway, and it provides a novel approach for the treatment of OA.

1. Introduction

Osteoarthritis (OA), a chronic joint disease, is characterized by damage and potential loss of articular cartilage and may be accompanied by bone hyperplasia.[1,2] According to statistics,[3] the global incidence and prevalence were approximately 86.7 million and 654.1 million respectively in 2020. Currently, the drugs for OA treatment are only limited to relieving symptoms, and there is no evidence indicating that they can repair cartilage and reverse joint damage, thus being unable to halt the progression of the disease.[4] Moreover, surgeries cannot be carried out for all patients.[5]

α-Ketoglutarate (AKG), a pivotal intermediate metabolite within the tricarboxylic acid (TCA) cycle, has been demonstrated to exert an impact on the level of reactive oxygen species (ROS) and the maintenance of immune system homeostasis (Fig. 1).[6] In cutaneous topical anti-inflammatory experiments,[7,8] AKG has exhibited remarkable anti-inflammatory efficacy. The underlying mechanisms of its action involve a mild reduction in the activity of the nutrient-sensing network,

* Corresponding author.
** Corresponding author.
E-mail addresses: shenhan@gdpu.edu.cn (H. Shen), 541608180@qq.com (L. Lu).
Peer review under the responsibility of Editorial Board of Journal of Holistic Integrative Pharmacy.

https://doi.org/10.1016/j.jhip.2025.02.003
Received 23 December 2024; Received in revised form 10 February 2025; Accepted 18 February 2025

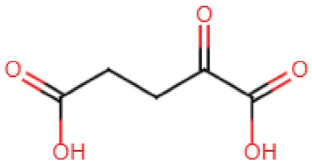

Fig. 1. The structure of α-ketoglutarate.

the elimination of senescent cells, and the enhancement of stem cell viability. Moreover, AKG plays a crucial role in multiple biological processes. It is involved in the regulation of stem cell differentiation, exerts anti-apoptotic effects, modulates the body's immune and inflammatory responses, contributes to muscle and bone development, and is essential for maintaining the stability of the cartilage matrix.[6,9,10] Based on these findings, we postulate that AKG may serve as a potential enhancer for augmenting the viability of mesenchymal stem cells (MSCs). Additionally, it holds promise as a protective agent for the repair of joint cartilage injury when combined with MSCs.

Currently, both platelet-rich plasma (PRP) and mesenchymal stem cells (MSCs) have been demonstrated to have protective effects on chondrocytes and can effectively repair damaged cartilage in OA. PRP, obtained by centrifuging whole blood, is a platelet-concentrated substance containing a high concentration of platelets and growth factors. It represents a potential treatment option for stimulating and accelerating regeneration in orthopedics.[11] MSCs, important members of the stem cell family, are adult stem cells. They are derived from the mesoderm and ectoderm in the early stage of development and can be isolated from various tissues such as bone marrow, adipose tissue, umbilical cord, endometrial polyps, and placenta.[12,13] MSCs maintain their multi-differentiation potential even after continuous passage culture and cryopreservation, making them suitable for clinical applications. They serve as ideal seed cells for the repair of tissue and organ damage caused by aging or diseases.[14] In the treatment of OA, MSCs can act through multiple mechanisms, including differentiating into chondrocytes, secreting growth factors and anti-inflammatory cytokines, and modulating the immune response.[15] When the dosage is relatively small, PRP shows significantly better therapeutic effects on OA than MSCs,[16] which was previously confirmed by our research group. However, as a blood-derived product, PRP has intractable problems in terms of product quality control and allogeneic application, and its long-term therapeutic effect gradually weakens. In contrast, MSCs do not have such limitations. However, MSCs in a senescent state or with an insufficient quantity in clinical settings may have reduced therapeutic efficacy. To overcome these challenges, we propose a novel strategy of combining AKG with MSCs for the treatment of OA.

The Hedgehog (HH) signaling pathway is a highly conserved intercellular signal-transduction system that transmits signals from the cell membrane to the nucleus. It plays a crucial role in embryonic development, cell proliferation, differentiation, and the maintenance of tissue homeostasis.[17,18] Studies have revealed that inhibiting the activity of the HH signaling pathway can, to some extent, slow down the progression of OA and alleviate the symptoms of patients.[19,20] Therefore, inhibiting the HH signaling pathway may represent a promising strategy for enhancing the treatment of OA.

Our study investigated the efficacy and underlying mechanisms of the combined application of AKG and MSCs in the treatment of OA. This treatment approach represents a novel strategy for treating OA.

2. Materials and methods

2.1. Cell culture with drug intervention

Subculture the cells at a ratio of 1:3. After the cells are subcultured to the P5 generation, conduct drug intervention with AKG. Subsequently, use a complete medium containing AKG for medium replacement in each subsequent subculture.

2.2. Observation of cell morphology

MSCs at P8 and P8 MSCs after AKG intervention were harvested and seeded into 6-well plates at a seeding density of 1×10^4 cells/well. The morphological changes of the cells were observed using an inverted fluorescence microscope after 72 h of culture. The number of senescent cells was counted using ImageJ software.

2.3. Scratch assay

Harvest P8 MSCs and P8 MSCs after AKG intervention, and seed them into 6-well plates at a seeding density of 5×10^5 cells/well. After the cell confluence reaches approximately 90%, quickly scratch the cells with a sterile pipette tip (200 μL). Replace the medium in the blank P8 group with a complete medium containing 0.25% FBS, and replace the medium in the experimental group with a complete medium containing AKG and 0.25% FBS. Take photos under an inverted fluorescence microscope at 0, 6, and 12 h respectively. Measure the scratch width using ImageJ software. Calculate the cell migration rate at each time-point. The formula for calculating the cell migration rate is as follows:

$$\text{Cell migration rate} = (\text{A-B})/\text{A} \times 100\%$$

(A: Initial scratch width; B: Scratch widths at 6 h and 12 h, respectively)

2.4. DAPI staining

Harvest P8 MSCs and P8 MSCs after AKG intervention, and seed them into a 24-well plate at a seeding density of 4×10^4 cells/mL. After 24 h of cell culture, wash the cells with PBS three times, 5 min each time. Fix the cells with 4% paraformaldehyde fixative for 30 min, then wash the cells with PBS three times, 5 min each time. Add DAPI staining solution and stain the cells in the dark for 5 min. After washing the cells with PBS three times, observe and take photos under an inverted fluorescence microscope. Count the number of apoptotic nuclei using ImageJ software.

2.5. AKG target screening

The correct structural formula of AKG was retrieved through the PubChem database (https://pubchem.ncbi.nlm.nih.gov). Then, it was imported into bioinformatics tools such as the Swiss Target Prediction database (http://swisstargetprediction.ch) and the PharmMapper database (https://www.lilab-ecust.cn/pharmmapper/) to collect the relevant predicted target protein and gene names. The Uniprot database (https://www.uniprot.org) was utilized to standardize the targets, with the species limited to "Homo sapiens".

2.6. OA target screening

OA-related gene loci were retrieved through the use of the subject term "Osteoarthritis" in the Gene Card database (https://www.genecards.org) and the OMIM database (https://www.omim.org).

2.7. Construction of drug-disease common targets and PPI network

Utilize the Venny database (https://bioinfogp.cnb.csic.es/tools/venny/) to display the intersection targets between AKG and OA in the form of a Venn diagram. Import the relevant gene targets obtained from the intersection by Venny into the STRING database (https://cn.string-db.org), with the species limited to "Homo sapiens", to obtain the protein-protein interaction (PPI) network diagram.

2.8. GO and KEGG enrichment analysis

Utilize the Metascape database (https://metascape.org/gp/index.html) to conduct Gene Ontology (GO) function and Kyoto Encyclopedia of Genes and Genomes (KEGG) pathway enrichment analyses. Select the results with significant difference ($P \leq 0.05$) for further analysis.

2.9. Molecular docking

Download the 2D structural information of AKG through the PubChem database. Search for and download the 3D protein structural information corresponding to the Indian Hedgehog (IHH), Patched 1 (PTCH-1), Smoothened (SMO), and Glioma-associated oncogene homolog 1 (GLI1) genes in the Protein Data Bank (PDB) database (https://www.rcsb.org/). Use the MOE software to remove water molecules and ligands from the proteins, conduct ligand-receptor molecular docking with the MOE software, and calculate the minimum binding free energy. Finally, use the PyMOL 2.5 software to construct the images of ligand-receptor molecular docking.

2.10. Animals

Forty male Sprague Dawley (SD) rats (7 weeks old) were obtained from the Guangdong Medical Laboratory Animal Center (Guangdong, China), the license number is SCXK (yue) 2022-0002. PRP was prepared using eight male SD rats (3 months old) obtained from Guangzhou Ruige Biotechnology Co., the license number is SCXK (yue) 2021-0059. Experiment protocols were approved by the Committee on Laboratory Animal Care and Use of Guangdong Pharmaceutical University (Guangzhou, China), in accordance with the National Institutes of Health guide for the care and use of laboratory animals (gdpulacspf2017691).

2.11. MIA-induced OA model

Currently, the methods available for establishing OA models in rodents include surgical and chemical interventions on the knee joint. Sodium iodoacetate (MIA) disrupts chondrocyte glycolysis by inhibiting glyceraldehyde-3-phosphate dehydrogenase, leading to chondrocyte death, neovascularization, subchondral bone necrosis and loss, as well as inflammation.[21] The pathological changes induced by MIA are similar to those of human OA. With its advantages of minimal invasiveness, reproducibility, and simplicity of operation, it has become the standard for simulating joint destruction in rat and mouse OA models. Based on the results of preliminary pre-experiments, the dosage of MIA selected for this experiment was determined to be 2 mg/50 μL (equivalent to a molar concentration of 0.1924 mM), and the modeling time was 14 days. After the modeling was completed, administration was carried out by intra-articular injection using a disposable syringe, once every 7 days for a total of 3 injections.

2.12. PRP preparation and activation

After anesthetizing the rats by intraperitoneal injection of 10% chloral hydrate, blood was collected from the heart. A 50 μL sample of whole blood was reserved for platelet counting. The remaining whole blood was added to sodium citrate anticoagulant and centrifuged at 1500 rpm for 15 min. Then, the upper-layer plasma was aspirated. After that, it was centrifuged at 3000 rpm for 20 min. Subsequently, 3/4 of the upper-layer liquid was discarded, and the remaining 1/4 of the liquid layer was PRP, which was resuspended by pipetting. PRP was mixed with 10% $CaCl_2$ containing 1000 U/mL thrombin at a volume ratio of 9:1. After activation at 37 °C for 1 h, the formed gel was gently mashed. Then, it was centrifuged at 4000 rpm for 10 min at 4 °C. The supernatant was collected for intra-articular injection in rats.

2.13. Preparation of AKG-combined MSCs solution

Digest the MSCs on the cell culture dish and transfer them to a centrifuge tube. Centrifuge at 1200 rpm for 5 min and discard the supernatant. Resuspend the cells with normal saline, and then take 10 μL of the cell suspension for counting. Next, centrifuge again at 1200 rpm for 5 min and discard the supernatant. Finally, add an equal-volume of AKG solutions with different concentrations to resuspend the cells, which are ready for use.

2.14. Grouping and drug treatment

Forty male SD rats were randomly divided into a control group, an MIA model group, a PRP positive control group, a low-dose AKG combined with mesenchymal stem cells (Low-dose AKG + MSCs) group, and a high-dose AKG combined with mesenchymal stem cells (High-dose AKG + MSCs) group. Each group was marked, and there were 8 rats in each group. After the rats in each group were adaptively fed for one week, their knee joints were used for the establishment of the OA model. Except that the knee joints of the rats in the control group and the MIA group were injected with 50 μL of normal saline, after the knee-joint modeling of the rats in the remaining groups was completed, intra-articular injection of therapeutic drugs was started. The injection volume was 50 μL, and the injection was carried out once every 7 days for 3 consecutive times. The positive control group received intra-articular injection of activated PRP. The Low-dose AKG + MSCs group received intra-articular injection of a suspension containing 10 mM AKG and 2.5×10^5 MSCs. The High-dose AKG + MSCs group received an intra-articular injection of a suspension containing 20 mM AKG and 2.5×10^5 MSCs. Previous research[22] has shown that the minimum injection dose of MSCs for the treatment of OA is $0.3 \times 10^6 - 2.7 \times 10^6$. In our study, the injection dose was reduced by one order of magnitude. The experimental procedure is shown in Fig. 2.

2.15. Gross observations

The right hind limbs of rats from each group were harvested. The muscles were carefully dissected away from the bones using surgical scissors, and then the femur and tibia were separated. The cartilage surface was observed and photographed under a stereomicroscope. The knee joint bone tissues were immersed in 4% paraformaldehyde and fixed for 24 h. The Pelletier score[23] was applied to the knee joint cartilage of each group to evaluate the degree of cartilage repair in the rat knee joints. The scoring criteria are shown in Table 1.

2.16. Histological examinations

The lateral and medial femoral condyles were fixed with 4% paraformaldehyde, decalcified with 10% EDTA, embedded in paraffin, and 4 μm microsections were prepared. These sections were stained with H&E, SO, and Masson's trichrome. Cartilage degeneration was evaluated according to the OARSI scoring system.[24] OARSI Total Score = Grade × Stage. The scoring criteria are shown in Tables 2 and 3.

2.17. Immunohistochemical (IHC) staining

According to the protocol of the SP Rabbit & Mouse HRP Kit, primary antibodies against IHH, SMO, GLI1, COL I, COL X, MMP-13, COL II, and ADAMTS-5 were used for incubating the bone tissue sections. After DAB staining, the sections were counterstained with hematoxylin and observed under a microscope. The ImageJ software was used to examine the percentage of positive cells.

2.18. Statistical analysis

Statistical analysis was performed using GraphPad 8.0 statistical

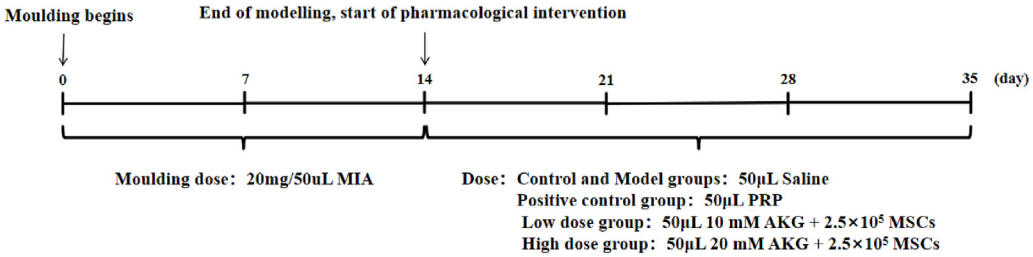

Fig. 2. Experimental procedure.

Table 1
Pelletier scoring standards.

Score	Performance
0	Normal articular cartilage surface
1	Roughness of the articular surface with small fissures
2	Erosion of the articular surface, with defects deep into the superficial or middle layer of cartilage
3	Ulceration of the articular surface with a deeper defect in the cartilage
4	Exfoliation of cartilage with exposure of subchondral bone

Table 2
OA cartilage histopathology grade assessment-advanced grading methodology.

Grade (Key Features)	Subgrade (Optional)	Performance
Grade 0: Intact surface cartilage	None	Intact cartilage
Grade 1: Intact surface	1.0 Intact cells 1.5 Cell death	Matrix: intact in the superficial area, edema and/or fibrillation; Cells: proliferation, hypertrophy, not just superficial fibrillation
Grade 2: Discontinuous surface	2.0 Fibrillation in the superficial area 2.5 Surface wear and matrix loss within the superficial layer	As above + Discontinuous surface, absence of cationic staining matrix in the upper 1/3 of cartilage
Grade 3: Vertical fissures	3.0 Simple fissures 3.5 Branching/complex fissures	As above + Cationic staining absent in 2/3 of the cartilage area
Grade 4: Erosion	4.0 Shallow delamination 4.5 Mid-layer cracking	Loss of cartilage matrix, cyst formation within the cartilage matrix
Grade 5: Denudation	5.0 Complete bone surface 5.5 Repaired tissue surface	The surface is sclerotic bone or repaired tissue, including fibrocartilage
Grade 6: Deformation	6.0 Osteophytes at the joint edge 6.5 Osteophytes at the joint edge and center	Bone remodeling, deformation of the joint surface contour Including: microcracks and repair

Table 3
OA cartilage histopathology-stage assessment.

Stage	Lesion Range (%)
0	None
1	<10%
2	10%–25%
3	25%–50%
4	>50%

software. For comparisons between two groups, the *t*-test (Student's test) was used. For comparisons among multiple groups, one-way analysis of variance (One-way ANOVA) was employed. A value of $P < 0.05$ was considered to indicate a statistically significant difference.

3. Result

3.1. AKG can enhance the activity of senescent MSCs

Normal MSCs are morphologically similar to fibroblasts, presenting various cell morphologies, mainly spindle-shaped. However, with the increase in the number of *in vitro* passages, obvious senescence phenomena occur in the cell morphology. For example, the cell body enlarges, the shape becomes broader and flatter, and the long-spindle shape is lost. The results of cell morphology observation (Fig. 3A and B) show that after AKG interference, compared with the P8 senescent MSCs group (P8 group), the number of senescent cells with such morphological characteristics decreased significantly ($P < 0.05$).

The results of the cell scratch assay (Fig. 3C and D) show that, compared with the P8 group, the scratches in the AKG group exhibited a significant tendency of healing at both 6 h and 12 h. This indicates that AKG can effectively enhance the viability of senescent MSCs in a short period and significantly promote the migration ability of senescent MSCs ($P < 0.05$).

In normal cells, nuclear staining appears uniform and the nuclear morphology is normal. However, in senescent cells, phenomena such as nuclear pyknosis and nuclear fragmentation occur, indicating that the cells are undergoing apoptosis. We used DAPI staining to detect cell apoptosis. The experimental results (Fig. 3E and F) show that, compared with the P8 group, the occurrences of nuclear pyknosis and nuclear fragmentation in the AKG group were reduced, and the apoptosis rate was significantly decreased ($P < 0.05$). This indicates that AKG can effectively reduce the apoptosis phenomenon of MSCs senescence caused by *in vitro* passages.

3.2. Bioinformatics analysis shows AKG is key in OA via the HH signaling pathway

We obtained 300 AKG targets from the Swiss Target Prediction and Pharm Mapper databases (Supplementary Tables 1–3), and 5336 OA targets from the Gene Card and OMIM databases (Supplementary Tables 4–5). Then, the intersection targets were obtained through a Venn diagram (Fig. 4A), and the Protein-Protein Interaction (PPI) network was presented by a network diagram (Fig. 4B).

To gain a better understanding of the regulatory role of AKG in OA, an analysis was conducted on the biological processes and signaling pathways of AKG's targets in regulating OA. Through the analysis of biological process (BP), molecular function (MF), and cellular component (CC) in Gene Ontology (GO) functions (Fig. 4C), it was found that AKG mainly regulates OA disease through embryonic development and tissue homeostasis. Meanwhile, when analyzing the results of the Kyoto Encyclopedia of Genes and Genomes (KEGG) pathways (Fig. 4C), we discovered that the HH signaling pathway was most closely related to skeletal development.[25] Therefore, we believe that regulating OA through the HH signaling pathway is the most appropriate.

For this purpose, molecular docking was conducted for further verification (Fig. 4D, Table 4). The results showed that the minimum binding

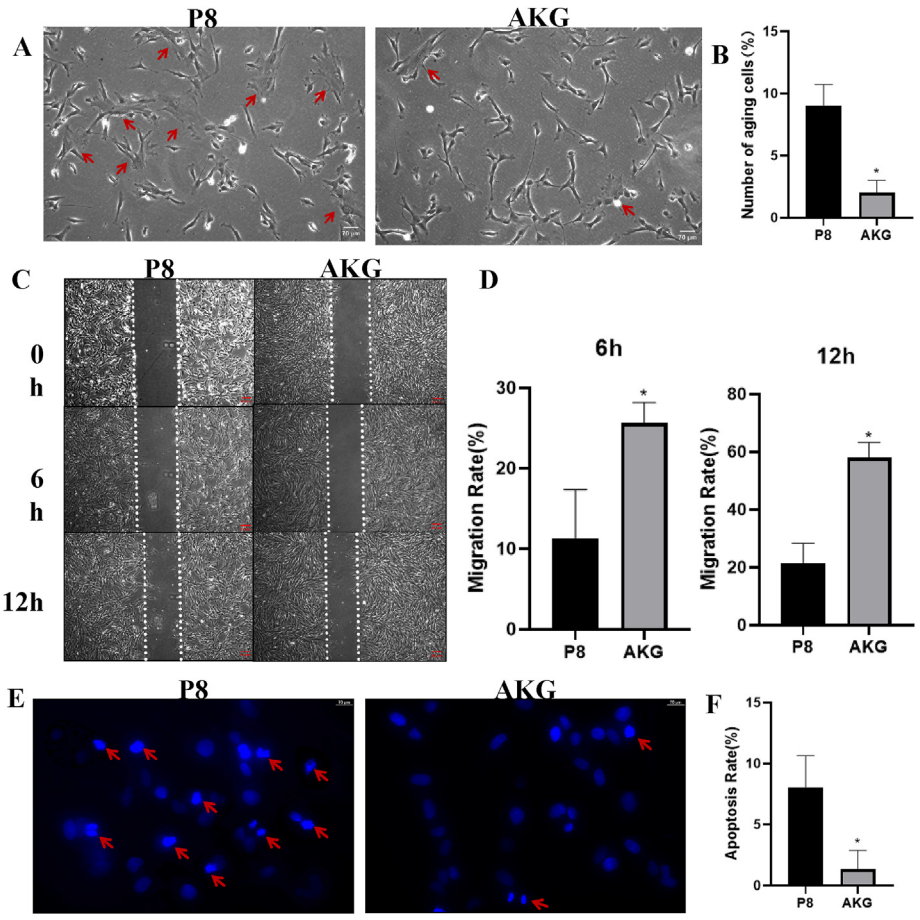

Fig. 3. AKG can enhance the activity of senescent MSCs. (A) Cell morphology images of the P8 group and the AKG group, respectively; (B) Quantification of the number of cells with senescent morphology; (C) Images of cell migration; (D) Cell migration rates at different time points; (E) Images of cell DAPI staining; (F) Quantification of cell apoptosis. All data are presented as the mean ± SD. *$P < 0.05$ vs Control group, n = 3.

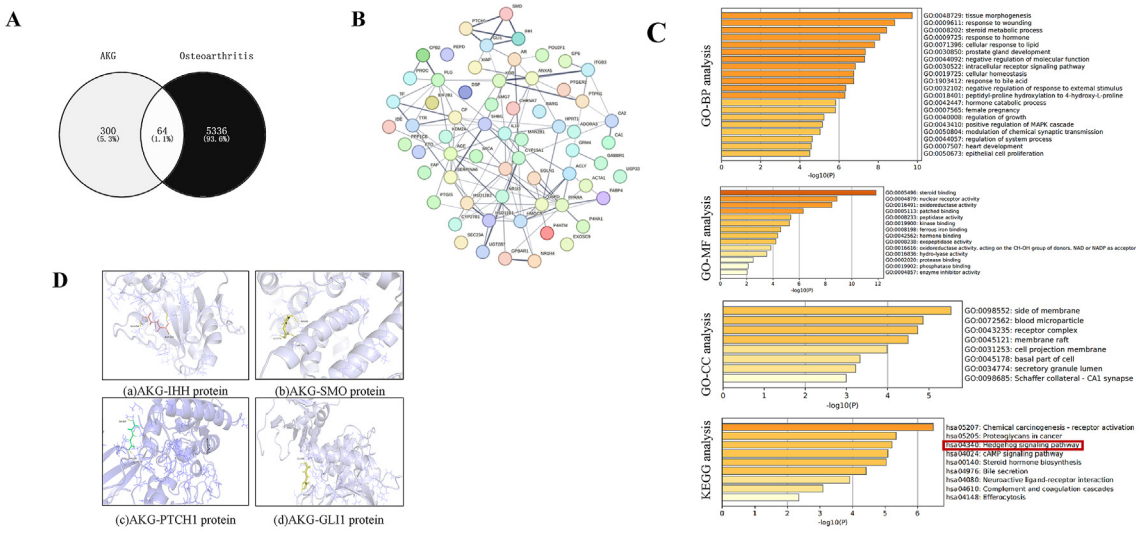

Fig. 4. Bioinformatics analysis shows AKG is key in OA via the HH signaling pathway. (A) Venn diagram depicting the intersection of AKG targets and OA targets. The gray region symbolizes the potential targets of AKG, the black region represents the potential targets associated with OA, and the white region denotes the common targets shared between the two. (B) PPI network diagram of the intersection between AKG and OA. (C) GO function and KEGG pathway enrichment analysis of AKG in relation to the potential OA targets. (D) Molecular docking outcomes of AKG with IHH, SMO, PTCH1, and GLI1 proteins.

free energies of AKG in molecular docking with IHH, PTCH-1, SMO, and GLI1 were −4.49 kcal/mol, −4.31 kcal/mol, −4.52 kcal/mol, and −4.48 kcal/mol respectively, and all had good binding affinities. This indicates that AKG can regulate OA by blocking the HH pathway.

Subsequently, animal experiments will be conducted to verify the feasibility of the combined application of AKG and MSCs on this pathway.

Table 4
Molecular docking results.

Target	Ligand	Docking score (the minimum binding free energy, kcal/mol)
IHH	AKG	−4.49
PTCH1	AKG	−4.31
SMO	AKG	−4.52
GLI1	AKG	−4.48

3.3. Combined medication synergistically alleviates cartilage destruction

We aimed to investigate the combined application of AKG and MSCs in counteracting the weakened function of MSCs with a relatively small quantity in the OA model and its impact on cartilage damage. The results of histomorphological observation (Fig. 5A) showed that the score of the MIA group (model group) was significantly higher than that of the control group ($P < 0.05$), and the score values of each drug-administration group were significantly lower than those of the MIA model group ($P < 0.05$), especially in the High-dose AKG + MSCs group (Fig. 5C).

HE, SO, and Masson staining revealed that in the control group, the surface of the knee joint cartilage was smooth without cracks, chondrocytes were neatly arranged, the cartilage structure was intact, and there was no loss of proteoglycans and collagen fibers. In the MIA group, the articular surface cartilage was eroded and replaced by thick layers of inflammatory fibrous tissue, severe cartilage fibrosis occurred, the arrangement of cells was disordered, and there were numerous hypertrophic chondrocytes in the deep zone, with a significant loss of proteoglycans and collagen fibers. In the drug-administration groups, the articular surface was intact, covered by a thin layer of fibrous tissue, and there were relatively fewer hypertrophic chondrocytes in the deep layer compared to the MIA group, along with a reduced loss of proteoglycans and collagen fibers (Fig. 5B). The OARSI scoring results demonstrated (Fig. 5D) that the score of the MIA group was significantly higher than that of the control group ($P < 0.05$). In contrast, the scores of the PRP group, the Low-dose AKG + MSCs group, and the High-dose AKG + MSCs group were significantly lower than those of the MIA group ($P < 0.05$). These results suggest that AKG can enhance the activity of MSCs and, when used in combination, prevent the joint cartilage destruction induced by MIA.

3.4. Combined medication synergistically inhibits the expression of hedgehog signaling

Research has shown[19] that inhibiting HH signal transduction can reduce the severity of OA. IHC staining showed that, compared with the control group, the administration with MIA significantly increased the number of cells positive for IHH, SMO, and GLI1. The PRP group effectively reduced the number of positive cells. The combined drug treatment group also reduced the expression levels of the downstream targets of the HH signaling pathway to varying degrees, and the high-dose group showed the best effect in particular (Fig. 6A and B, $P < 0.05$). This has confirmed that the synergistic effect of AKG combined with MSCs can reduce the expression of the HH signaling pathway activated by OA damage induced by MIA.

3.5. Combined medication synergistically improves ECM metabolic homeostasis in articular cartilage

Type II collagen (COL II) serves as the structural framework of the chondrocyte extracellular matrix (ECM).[26] Type X collagen (COL X) further induces the expression of articular cartilage matrix-degrading enzymes (MMP-13 and ADAMTS-5) during the progression of OA. Observation by IHC staining revealed that, compared with the control group, the administration with MIA significantly reduced the number of COL II positive cells, while significantly increasing the number of COL X, MMP-13, and ADAMTS-5 positive cells. Compared with the MIA group, the treatment in the PRP group significantly increased the number of COL II positive cells, but significantly decreased the number of COL X, MMP-13, and ADAMTS-5 positive cells. The combined drug treatment groups with different dosages all showed significant restorative effects against the MIA treatment, and the high-dose group showed the best effect in particular (Fig. 7A and B, $P < 0.05$). This indicates that the combined medication can effectively maintain the metabolic balance of the ECM in the MIA-induced damaged articular cartilage.

3.6. Combined medication synergistically reduces endochondral ossification in articular cartilage

When cartilage is replaced by bone, the expression of Type I collagen (COL I) is activated.[27] Its abnormal expression may participate in the pathological process of endochondral ossification by affecting biological processes such as the proliferation, differentiation, and apoptosis of articular chondrocytes.[28] Observation by IHC staining revealed that, compared with the control group, the administration with MIA significantly increased the number of COL I positive cells. The treatment in the PRP group significantly decreased the number of COL I positive cells. The combined drug treatment groups with different dosages all showed significant restorative effects against the MIA treatment, and the high-dose group showed the best effect in particular (Fig. 8A and B, $P < 0.05$). This indicates that the combined medication can effectively reduce endochondral ossification in the MIA-induced damaged articular cartilage.

4. Discussion

Osteoarthritis is a progressive joint disorder, typically characterized by the destruction of articular cartilage and subchondral bone. MSCs, adult stem cells with multi-directional differentiation potential, are key research subjects in tissue engineering and regenerative medicine. Yet, with more passages, their proliferation weakens and senescence becomes obvious, reducing biological activity and clinical effectiveness. Some studies show that cell proliferation declines and senescent morphologies emerge at P8 *in vitro*.[29] In osteoarthritis treatment, senescent MSCs may not offer enough cells or chondrocytes for cartilage repair. During senescence, the apoptosis rate of MSCs rises, and they can't recruit macrophages effectively or polarize them to the M2 phenotype, increasing SASP factors and causing immune and inflammatory responses.[30] Improving MSCs' *in vitro* passaging senescence can enhance their vitality and repair ability for tissue diseases.

Quan and his colleagues disclosed that AKG exerted a significant role in regulating skeletal disorders.[6] Nevertheless, its role and molecular mechanism in the treatment of OA remain to be elucidated. In this study, the pharmacological mechanism of AKG in the treatment of OA was investigated via bioinformatics analysis. We performed a GO functional enrichment analysis on the candidate targets of AKG in the treatment of OA. The functions enriched by these targets are intimately associated with cell proliferation, differentiation, and apoptosis. Through KEGG pathway enrichment analysis, it was revealed that this could be related to the HH signaling pathway. Consequently, we employed molecular docking technology to simulate and hypothesize the binding scenario between AKG and the proteins associated with the HH signaling pathway in OA. This pathway is implicated in the over-hypertrophy of chondrocytes, which in turn contributes to the degeneration of articular cartilage. It was demonstrated that AKG could impede the progression of OA through the HH signaling pathway. Subsequently, we applied the identified pathway to animal experiments for validation. In the existing research field of OA treatment, most studies are concentrated on single drug or cell therapies. However, exploring the combination of AKG with a small amount of MSC and delving into the HH signaling pathway is an innovative research approach. Through the targeted regulation of the signaling pathway, it provides a new perspective for revealing the pathogenesis and therapeutic targets of osteoarthritis, and helps to improve the theoretical system of the pathophysiological mechanism of OA.

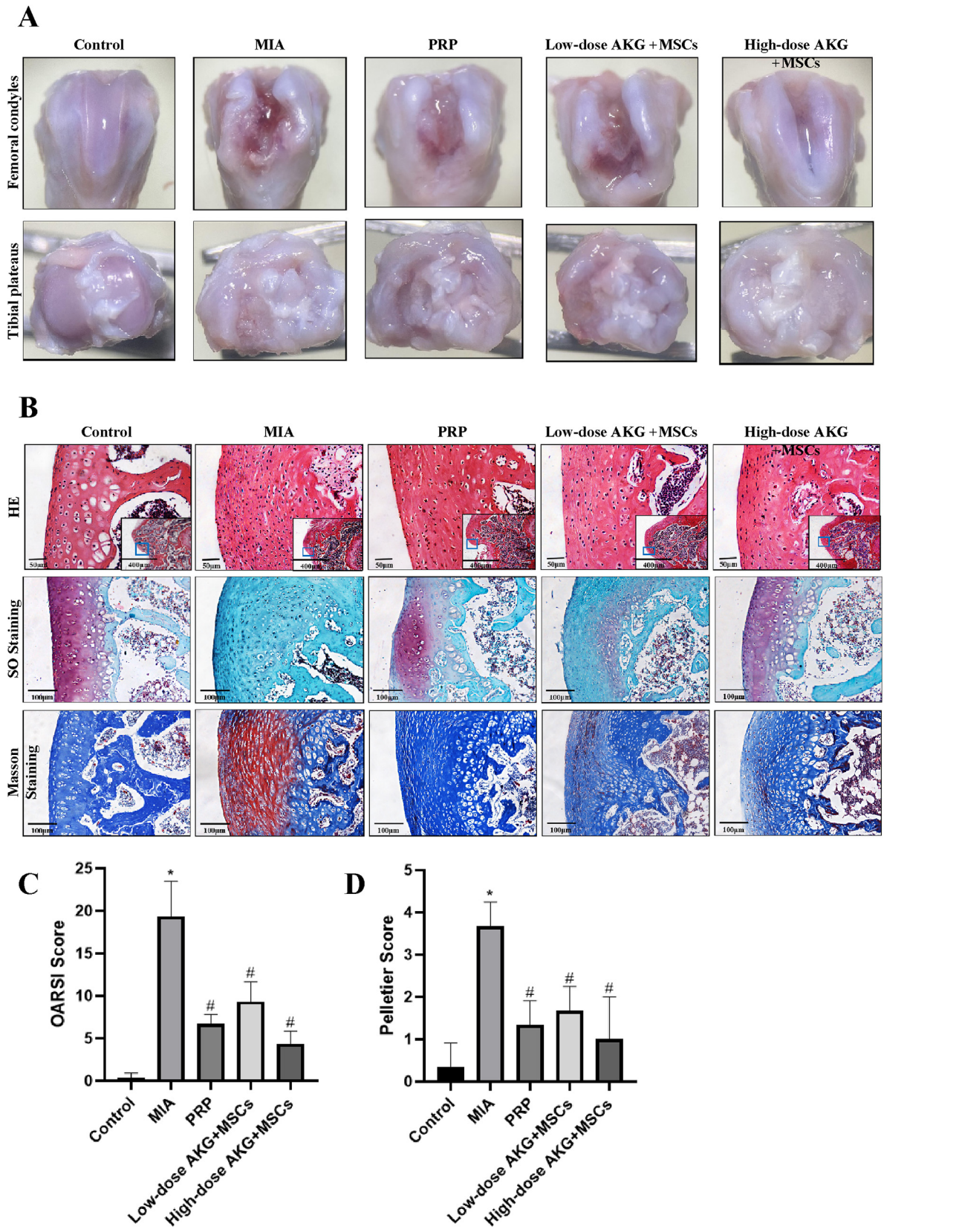

Fig. 5. Combined medication synergistically alleviates cartilage destruction. (A) Morphologic observation of articular cartilage repair. (B) HE, SO, and Masson staining. (C) Pelletier score. (D) Statistical analysis of OARSI score. All data are presented as the mean ± SD. $^{*}P < 0.05$ vs Control group; $^{\#}P < 0.05$ vs MIA group, n = 3.

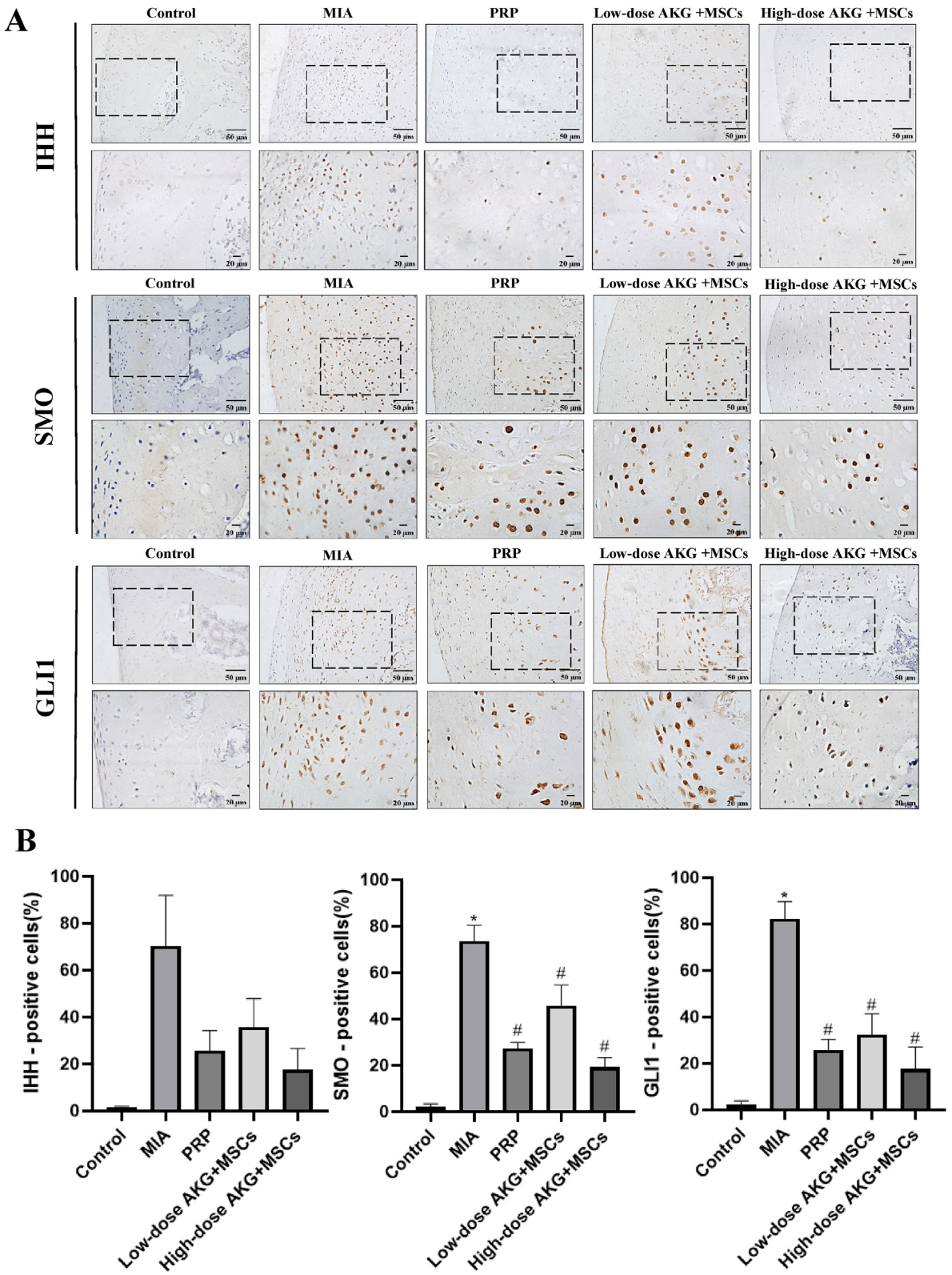

Fig. 6. Combined medication synergistically inhibits the expression of Hedgehog signaling. (A) Immunohistochemical staining of IHH, SMO, and GLI1 in articular cartilage. (B) Quantification of IHH, SMO, and GLI1 positive cells in articular cartilage. All data are presented as the mean ± SD. $^{*}P < 0.05$ vs Control group; $^{\#}P < 0.05$ vs MIA group, n = 3.

In this study, we induced a rat model of osteoarthritis through intra-articular injection of MIA. This method is classified as a secondary OA model induced by specific factors. MIA is a well-known inhibitor of glycerol-3-phosphate dehydrogenase. Injecting MIA into the knee joint cavity can increase the cellularity of chondrocytes. The proliferating chondrocytes then secrete pro-inflammatory cytokines and tissue-destroying enzymes, leading to abnormal metabolism in the articular cartilage microenvironment along with excessive inflammation.

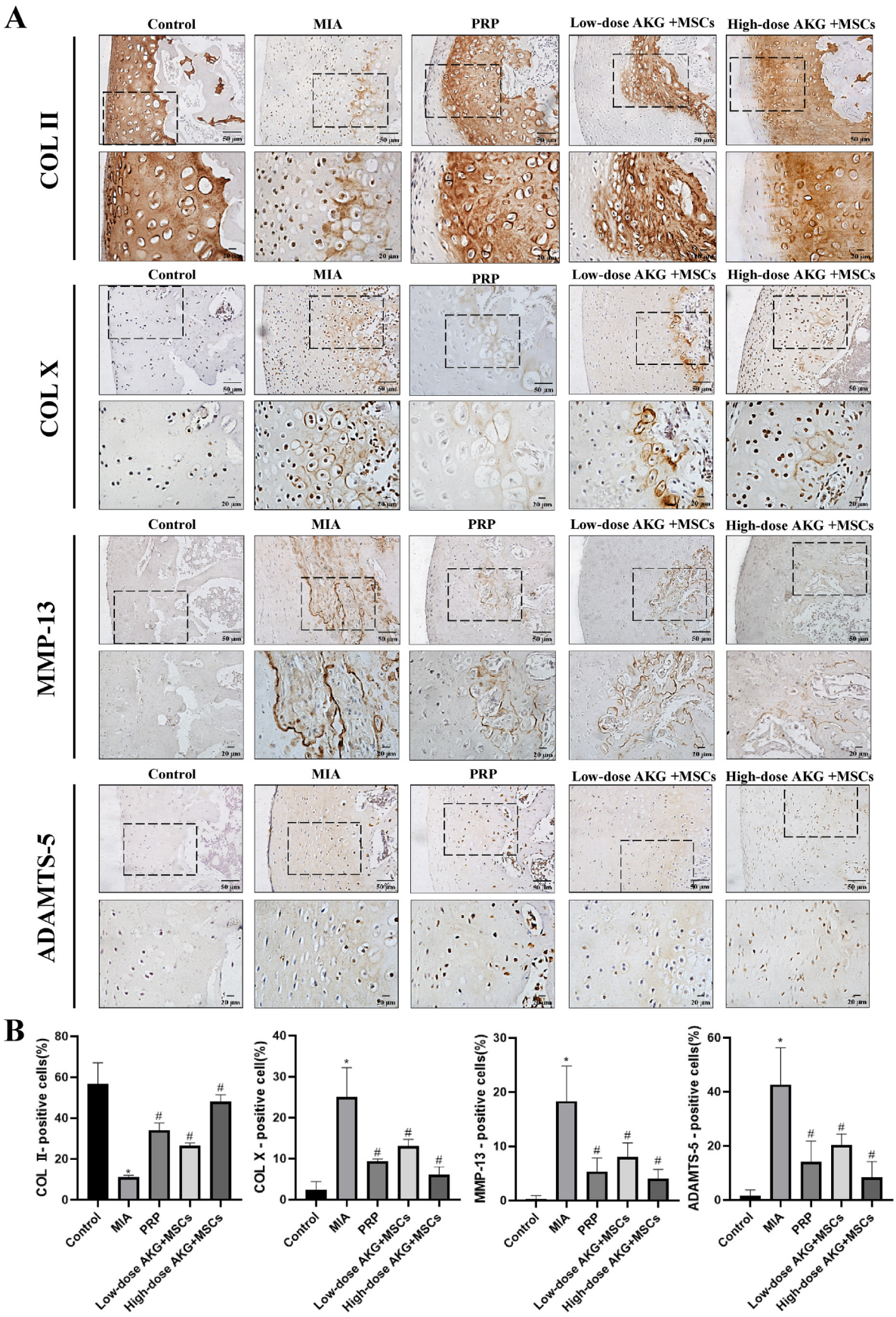

Fig. 7. Combined medication synergistically improves ECM metabolic homeostasis in articular cartilage. (A) Immunohistochemical staining of COL II, COL X, MMP-13, and ADAMTS-5 in articular cartilage. (B) Quantification of COL II, COL X, MMP-13, and ADAMTS-5 positive cells in articular cartilage. All data are presented as the mean ± SD. $^{*}P < 0.05$ vs Control group; $^{\#}P < 0.05$ vs MIA group, n = 3.

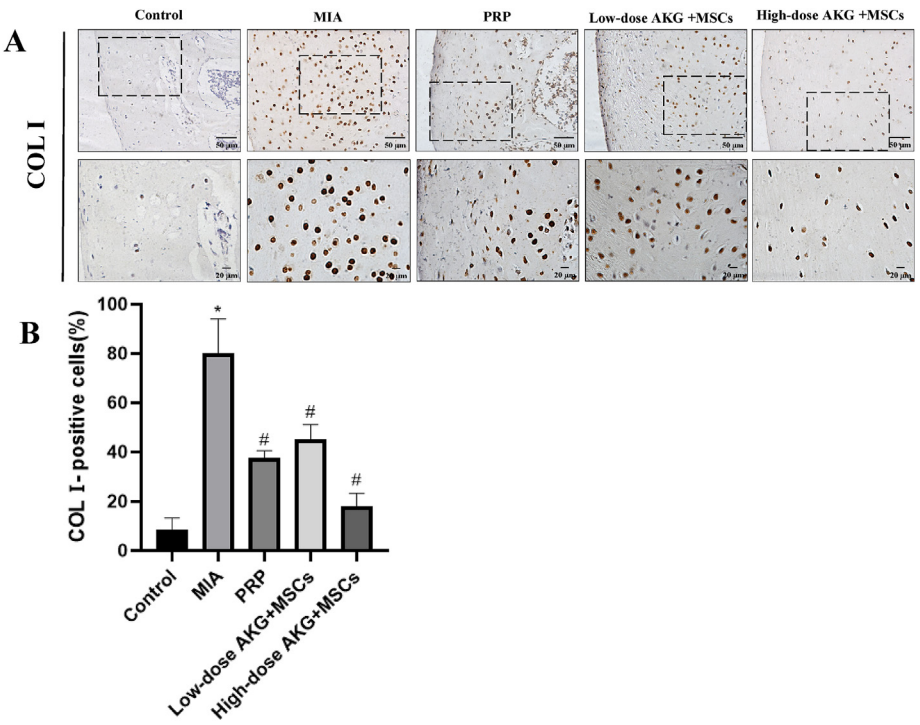

Fig. 8. Combined medication synergistically reduces endochondral ossification of articular cartilage. (A) Immunohistochemical staining of COL I in articular cartilage. (B) Quantification of COL I positive cells in articular cartilage. All data are presented as the mean ± SD. $^{*}P < 0.05$ vs Control group; $^{\#}P < 0.05$ vs MIA group, n = 3.

Eventually, this results in joint instability, such as cartilage degradation and degeneration.[31] In our experiment, morphological examination of the articular cartilage revealed that in the MIA group, the cartilage of the tibial plateau and femoral condyle was severely damaged, with obvious ulcer formation and even exposure of subchondral bone. In contrast, the degree of articular cartilage damage in the combined administration groups with different doses was alleviated to varying degrees. This indicates that the administration of AKG combined with MSCs at high and low doses can promote cartilage repair in osteoarthritic rats to different extents.

We explored the repair effect of the administration of AKG combined with MSCs at high and low doses on articular cartilage from the perspective of the pathological changes in OA. By analyzing the results of three pathological staining methods and comparing them with normal articular cartilage, we found that the main pathological features of the articular cartilage in osteoarthritic rats induced by MIA included: on one hand, the surface of the articular cartilage was eroded by thick layers of inflammatory fibrous tissue, with severe cartilage fibrosis; on the other hand, a large number of chondrocytes in the deep zone near the subchondral bone showed a hypertrophic state. Cartilage fibrosis and hypertrophy are hallmark features of OA, which lead to the loss of proteoglycans and collagen fibers in the cartilage matrix. As a result, the integrity and stability of the cartilage matrix are compromised, further promoting articular cartilage damage. In this study, the administration of AKG combined with MSCs could effectively inhibit cartilage surface fibrosis and reduce deep-layer cartilage hypertrophy, improve the loss of proteoglycans and collagen fibers in the cartilage matrix, and thus had a significant repair effect on articular cartilage.

HH signaling pathway is one of the key regulatory factors in metazoan development and has been demonstrated to play a crucial role in many developmental and physiological processes. However, its abnormal activation can easily trigger a variety of human diseases, such as OA.[25,32] The HH signaling pathway exerts different regulatory functions mainly through various ligands. Specifically, IHH mainly acts on the development of bones and joints.[33] When the IHH signal is present, the SMO membrane protein is released, which promotes the activated GLI transcription factor to enter the nucleus, thereby increasing the transcription level of downstream proteins. This, in turn, regulates chondrocyte proliferation, differentiation, and bone formation, and influences the development of bones and cartilage.[34]

Once activated, the HH pathway causes chondrocytes to exhibit abnormal fibrotic and hypertrophic morphologies, accelerating cartilage calcification and endochondral ossification. This process contributes to the progression of OA and leads to cartilage degeneration in the body. Research has shown that transgenic mice with induced over-expression of IHH display characteristics similar to human OA, such as increased chondrocyte hypertrophy and cartilage damage.[19,35] Conversely, conditional targeted inhibition of IHH in chondrocytes of osteoarthritic rats can alleviate disease symptoms such as articular cartilage destruction, subchondral bone degradation, and synovial inflammation.[36] Activating the HH pathway inhibits the expression of chondrocyte-specific proteins, COL II and proteoglycans, and induces an increase in the expression of COL X, a marker of chondrocyte hypertrophy. It also promotes the expression of matrix-degrading enzymes (MMPs and ADAMTS-5) and increases the expression of COL I, a marker of osteoblasts, thus accelerating the osteogenesis process. Ultimately, this leads to aggravated articular cartilage damage and skeletal dysplasia.[37,38] Therefore, the HH signal is a key pathway in the progression of OA, and blocking this signal is beneficial for preventing and treating articular cartilage degeneration in OA.

SMO and GLI1 are key proteins in the HH signaling pathway. In this study, the articular chondrocytes of osteoarthritic rats induced by MIA showed high expression of SMO and GLI1, indicating that the HH pathway was activated in the articular chondrocytes of these rats, which is consistent with previous research findings.[39,40] The administration of AKG combined with MSCs could inhibit the expression of SMO and GLI1 in chondrocytes, suggesting that this combined administration has an inhibitory effect on the activation of the HH pathway in chondrocytes.

COL II is a typical collagen secreted by normal chondrocytes, providing elasticity and toughness to cartilage. COL X is mainly expressed in hypertrophic chondrocytes during the growth and development of cartilage and serves as a marker of chondrocyte hypertrophy. COL I is the

main collagen component in bones and can promote the activity of osteoblasts. In osteoarthritic articular cartilage, a reduction in the synthesis and metabolism of COL II may affect the expression and distribution of COL X. Since COL II provides structural support for cartilage, its decrease can lead to changes in the cartilage environment, thereby influencing the normal function of COL X.[41] However, in the context of OA, this expression pattern is altered. As the disease progresses, the level of COL X is abnormally elevated. Its over-expression promotes chondrocyte hypertrophy and abnormal matrix calcification. These chondrocytes are further transformed into osteoblasts, destroying the normal structure of cartilage and accelerating endochondral ossification.[28,42] As the main collagen component in bones,[43] COL I is essential for osteogenesis in OA. When OA occurs, the damage to articular cartilage stimulates the repair response of surrounding tissues, with osteogenic activity being an important part. The increased synthesis of COL I provides the necessary structural support for the formation of new bone, endowing the newly formed bone tissue with strength and stability.[44] Meanwhile, factors such as inflammatory cytokines and mechanical stimulation can further promote the expression of COL I, accelerating the osteogenesis process.[45,46] However, excessive osteogenesis is not favorable, as it may lead to the formation of osteophytes. These abnormal bone growths can affect the normal movement of joints and exacerbate the symptoms of OA.[47] In this study, the expression of COL II in the articular cartilage of OA rats induced by MIA was significantly decreased, while the positive expressions of COL I and COL X were remarkably increased, further demonstrating the gradual hypertrophy of articular cartilage and endochondral ossification. The administration of AKG combined with MSCs could significantly enhance the expression of COL II in chondrocytes and inhibit the expression of COL I and COL X, indicating that it can effectively inhibit the excessive hypertrophy of OA articular chondrocytes and endochondral ossification.

ADAMTS-5 and MMP-13 are markers of articular cartilage matrix degradation. ADAMTS-5 can degrade aggrecan in articular cartilage. Aggrecan is crucial for maintaining the structure and function of cartilage. When ADAMTS-5 is over-expressed, it will accelerate the degradation of aggrecan and disrupt the integrity of cartilage.[48] MMP-13 is mainly responsible for degrading COL II in the cartilage matrix.[49] COL II is one of the main components of cartilage, providing strength and elasticity to it. An abnormal increase in MMP-13 will lead to excessive degradation of COL II, causing cartilage to lose its proper mechanical properties.[50] In this study, AKG combined with MSCs could effectively inhibit the expression of ADAMTS-5 and MMP-13 in the articular cartilage of OA rats, improve cartilage matrix degradation, and promote chondrocytes to secrete COL II and aggrecan.

From the aforementioned results, the combination of AKG's regulation of cellular metabolism with the multi-directional differentiation and immunomodulatory functions of MSC is likely to generate a synergistic effect. This combined treatment modality targets the complex pathological processes of OA, including cartilage damage, inflammatory responses, and extracellular matrix imbalance, in a more comprehensive manner than a single therapy, thereby providing potential for enhancing treatment outcomes.

However, the current study has several limitations. Existing research lacks long-term follow-up of rats treated with AKG and a small amount of MSC. As time passes, the inflammation induced by MIA may recur or become chronic. Moreover, the sustained efficacy of the AKG and MSC combination and the possibility of new adverse reactions remain unclear. This significantly impedes the translation of this treatment approach into clinical practice, where a thorough understanding of the treatment's long-term safety and stability is essential.

5. Conclusion

This study found that AKG could enhance the activity of MSCs. In an MIA-induced OA rat model, intra-articular injection of AKG combined with MSCs can significantly inhibit the degenerative changes of articular cartilage. This protective effect is derived from the inhibition of the activation of the HH signaling pathway in chondrocytes. This finding provides a new potential strategy for the treatment of OA. The results of this study lay the foundation for further exploring the molecular mechanism of the treatment of OA with AKG combined with MSCs. Follow-up studies can deeply analyze the specific roles of each component in this combination therapy and their synergistic mechanisms to optimize the treatment plan. If it can be verified in more animal models and subsequent clinical trials, the treatment with AKG combined with MSCs is expected to become a safe and effective new method for the treatment of OA, bringing new hope to a large number of OA patients, relieving their pain, and improving their quality of life.

CRediT authorship contribution statement

Liyan Li: Writing – original draft, Software, Methodology, Investigation, Formal analysis, Data curation. **Han Shen:** Writing – review & editing, Supervision, Conceptualization. **Li Lu:** Writing – review & editing, Supervision.

Ethic statement

Experiment protocols were approved by the Committee on Laboratory Animal Care and Use of Guangdong Pharmaceutical University (Guangzhou, China), in accordance with the National Institutes of Health guide for the care and use of laboratory animals (gdpulacspf2017691).

Data availability statement

The data that support the findings of this study are available from the corresponding authors upon reasonable request.

Funding

This study was supported by the Natural Science Foundation of Guangdong Province (NO. 2024A1515010873).

Declaration of competing interest

The authors declare that they have no competing interests.

Appendix A. Supplementary data

Supplementary data to this article can be found online at https://doi.org/10.1016/j.jhip.2025.02.003.

References

1. Hayami T, Pickarski M, Zhuo Y, et al. Characterization of articular cartilage and subchondral bone changes in the rat anterior cruciate ligament transection and meniscectomized models of osteoarthritis. *Bone*. 2006;38(2):234–243.
2. Li Q, Hou C, Zhang P, et al. A network pharmacology study on the main active constituents and key pharmacological pathways of Shaoyao Gancao decoction on osteoarthritis. *J Holist Integr Pharm*. 2021;2(1):56–68.
3. Shumnalieva R, Kotov G, Monov S. Obesity-related knee osteoarthritis—current concepts. *Life*. 2023;13(8):1650.
4. Barnes EV, Edwards NL. Treatment of osteoarthritis. *South Med J*. 2005;98(2):205–209.
5. Gramstad GD, Galatz LM. Management of elbow osteoarthritis. *J Bone Joint Surg Am*. 2006;88(2):421–430.
6. Wang Y, Deng P, Liu Y, et al. Alpha-ketoglutarate ameliorates age-related osteoporosis via regulating histone methylations. *Nat Commun*. 2020;11(1):5596.
7. Yang F, Zhou Z, Guo M, et al. The study of skin hydration, anti-wrinkles function improvement of anti-aging cream with alpha-ketoglutarate. *J Cosmet Dermatol*. 2022;21(4):1736–1743.
8. Li S, Zhao C, Shang G, et al. α-Ketoglutarate preconditioning extends the survival of engrafted adipose-derived mesenchymal stem cells to accelerate healing of burn wounds. *Exp Cell Res*. 2024;439(1):114095.
9. Liu S, Yang J, Wu Z. The regulatory role of α-ketoglutarate metabolism in macrophages. *Mediators Inflamm*. 2021;2021:1–7.

10. Ye X, Li X, Qiu J, et al. Alpha-ketoglutarate ameliorates age-related and surgery induced temporomandibular joint osteoarthritis via regulating IKK/NF-κB signaling. *Aging Cell*. 2024;23(11):e14269.
11. Rodriguez-Merchan EC. Intraarticular injections of platelet-rich plasma (PRP) in the management of knee osteoarthritis. *Arch Bone Joint Surg*. 2013;1(1):5–8.
12. Gugjoo MB, Amarpal A, Sharma GT. Mesenchymal stem cell basic research and applications in dog medicine. *J Cell Physiol*. 2019;234(10):16779–16811.
13. Ding DC, Shyu WC, Lin SZ. Mesenchymal stem cells. *Cell Transplant*. 2011;20(1):5–14.
14. Mamidi MK, Nathan KG, Singh G, et al. Comparative cellular and molecular analyses of pooled bone marrow multipotent mesenchymal stromal cells during continuous passaging and after successive cryopreservation. *J Cell Biochem*. 2012;113(10):3153–3164.
15. Primorac D, Molnar V, Rod E, et al. Knee osteoarthritis: a review of pathogenesis and state-of-the-art non-operative therapeutic considerations. *Genes*. 2020;11(8):854.
16. Zhao J, Liang G, Han Y, et al. Combination of mesenchymal stem cells (MSCs) and platelet-rich plasma (PRP) in the treatment of knee osteoarthritis: a meta-analysis of randomised controlled trials. *BMJ Open*. 2022;12(11):e061008.
17. Mcmillan R, Matsui W. Molecular pathways: the hedgehog signaling pathway in cancer. *Clin Cancer Res*. 2012;18(18):4883–4888.
18. Jing J, Wu Z, Wang J, et al. Hedgehog signaling in tissue homeostasis, cancers and targeted therapies. *Signal Transduct Target Ther*. 2023;8(1):315.
19. Lin AC, Seeto BL, Bartoszko JM, et al. Modulating hedgehog signaling can attenuate the severity of osteoarthritis. *Nat Med*. 2009;15(12):1421–1425.
20. Fazio A, Di Martino A, Brunello M, et al. The involvement of signaling pathways in the pathogenesis of osteoarthritis: an update. *J Orthop Transl*. 2024;47:116–124.
21. Pitcher T, Sousa-Valente J, Malcangio M. The monoiodoacetate model of osteoarthritis pain in the mouse. *J Vis Exp*. 2016;(111):53746.
22. Koh YG, Jo SB, Kwon OR, et al. Mesenchymal stem cell injections improve symptoms of knee osteoarthritis. *Arthroscopy J Arthrosc Relat Surg*. 2013;29(4):748–755.
23. Pelletier JP, Jovanovic D, Fernandes JC, et al. Reduced progression of experimental osteoarthritis *in vivo* by selective inhibition of inducible nitric oxide synthase. *Arthritis Rheum*. 1998;41(7):1275–1286.
24. Pritzker KPH, Gay S, Jimenez SA, et al. Osteoarthritis cartilage histopathology: grading and staging. *Osteoarthr Cartil*. 2006;14(1):13–29.
25. Xiao W, Li Y, Deng A, et al. Functional role of hedgehog pathway in osteoarthritis. *Cell Biochem Funct*. 2020;38(2):122–129.
26. Bay-Jensen AC, Mobasheri A, Thudium CS, et al. Blood and urine biomarkers in osteoarthritis – an update on cartilage associated type II collagen and aggrecan markers. *Curr Opin Rheumatol*. 2022;34(1):54–60.
27. Fujii Y, Liu L, Yagasaki L, et al. Cartilage homeostasis and osteoarthritis. *Int J Mol Sci*. 2022;23(11):6316.
28. Li B, Guan G, Mei L, et al. Pathological mechanism of chondrocytes and the surrounding environment during osteoarthritis of temporomandibular joint. *J Cell Mol Med*. 2021;25(11):4902–4911.
29. Luo S, Xiao S, Ai Y, et al. Changes in the hepatic differentiation potential of human mesenchymal stem cells aged in vitro. *Ann Transl Med*. 2021;9(21), 1628-1628.
30. Fraile M, Eiro N, Costa LA, et al. Aging and mesenchymal stem cells: basic concepts, challenges and strategies. *Biology*. 2022;11(11):1678.
31. Kwon M, Nam D, Kim J. Pathological characteristics of monosodium iodoacetate-induced osteoarthritis in rats. *Tissue Eng Regen Med*. 2023;20(3):435–446.
32. Lee RTH, Zhao Z, Ingham PW. Hedgehog signalling. *Development*. 2016;143(3):367–372.
33. Dilower I, Niloy AJ, Kumar V, et al. Hedgehog signaling in gonadal development and function. *Cells*. 2023;12(3):358.
34. Sun Q, Huang J, Tian J, et al. Key roles of Gli1 and Ihh signaling in craniofacial development. *Stem Cells Dev*. 2024;33(11-12):251–261.
35. Zhou J, Wei X, Wei L. Indian Hedgehog, a critical modulator in osteoarthritis, could be a potential therapeutic target for attenuating cartilage degeneration disease. *Connect Tissue Res*. 2014;55(4):257–261.
36. Huang L, Jin M, Gu R, et al. miR-199a-5p reduces chondrocyte hypertrophy and attenuates osteoarthritis progression via the Indian Hedgehog signal pathway. *J Clin Med*. 2023;12(4):1313.
37. Luan J, Tao H, Su Y. Taladegib controls early chondrocyte hypertrophy via inhibiting smoothened/Gli1 pathway. *Am J Transl Res*. 2020;12(5):1985–1993.
38. Renaudin F, Oudina K, Gerbaix M, et al. NADPH oxidase 4 deficiency attenuates experimental osteoarthritis in mice. *RMD Open*. 2023;9(1):e002856.
39. Li P, Gao Y, Zhou R, et al. Intra-articular injection of miRNA-1 agomir, a novel chemically modified miRNA agonists alleviates osteoarthritis (OA) progression by downregulating Indian hedgehog in rats. *Sci Rep*. 2024;14(1):8101.
40. Weber AE, Lymfat S, Lalali O, et al. Kappa opioids modulate hedgehog signaling to attenuate osteoarthritis. *Osteoarthr Cartilage*. 2020;28:S189.
41. Marlina M, Rahmadian R, Armenia A, et al. Conditioned medium of IGF1-induced synovial membrane mesenchymal stem cells increases chondrogenic and chondroprotective markers in chondrocyte inflammation. *Biosci Rep*. 2021;41(7):BSR20202038.
42. Masutani T, Yamada S, Hara A, et al. Exogenous application of proteoglycan to the cell surface microenvironment facilitates to chondrogenic differentiation and maintenance. *Int J Mol Sci*. 2020;21(20):7744.
43. Andre G, Chretien A, Demoulin A, et al. Col1A-2 mutation in osteogenesis imperfecta mice contributes to long bone fragility by modifying cell-matrix organization. *Int J Mol Sci*. 2023;24(23):17010.
44. Maurotti S, Mare R, Pujia R, et al. Hemp seeds in post-arthroplasty rehabilitation: a pilot clinical study and an *in vitro* investigation. *Nutrients*. 2021;13(12):4330.
45. Li Z, Xie L, Zeng H, et al. PDK4 inhibits osteoarthritis progression by activating the PPAR pathway. *J Orthop Surg Res*. 2024;19(1):109.
46. Luo P, Yuan Q, Wan X, et al. Effects of immune cells and cytokines on different cells in OA. *J Inflamm Res*. 2023;16:2329–2343.
47. Zhang L, Wen C. Osteocyte dysfunction in joint homeostasis and osteoarthritis. *Int J Mol Sci*. 2021;22(12):6522.
48. Xiang W, Wang C, Zhu Z, et al. Inhibition of SMAD3 effectively reduces ADAMTS-5 expression in the early stages of osteoarthritis. *BMC Musculoskelet Disord*. 2023;24(1):169.
49. Yunus MHM, Nordin A, Kamal H. Pathophysiological perspective of osteoarthritis. *Medicina*. 2020;56(11):614.
50. Hu Q, Ecker M. Overview of MMP-13 as a promising target for the treatment of osteoarthritis. *Int J Mol Sci*. 2021;22(4):1742.